

1 Soil CO₂ efflux and production rates as influenced by evapotranspiration in a dry grassland

2
3 János Balogh^{a,b,*}, Szilvia Fóti^c, Krisztina Pintér^a, Susanne Burri^b, Werner Eugster^b, Marianna Papp^c
4 and Zoltán Nagy^{a,c}

5 ^aInstitute of Botany and Ecophysiology, Szent István University, Páter u. 1, 2100 Gödöllő, Hungary

6 ^bGrassland Sciences Group, Institute of Agricultural Sciences, ETH Zurich, Universitätsstrasse 2,
7 8092 Zürich, Switzerland

8 ^cMTA-SZIE Plant Ecology Research Group, Szent István University, Páter K. u. 1, 2103 Gödöllő,
9 Hungary

10 11 **Abstract**

12 *Aims* Our aim was to study the effect of potential biotic drivers, including evapotranspiration (ET)
13 and gross primary production (GPP), on the soil CO₂ production and efflux on the diel time scale.

14 *Methods* Eddy covariance, soil respiration and soil CO₂ gradient systems were used to measure the
15 CO₂ and H₂O fluxes in a dry, sandy grassland in Hungary. The contribution of CO₂ production from
16 three soil layers to plot-scale soil respiration was quantified. CO₂ production and efflux residuals
17 after subtracting the effects of the main abiotic and biotic drivers were analysed.

18 *Results* Soil CO₂ production showed a strong negative correlation with ET rates with a time lag of
19 0.5 hours in the two upper layers, whereas less strong, but still significant time-lagged and positive
20 correlations were found between GPP and soil CO₂ production. Our results suggest a rapid negative
21 response of soil CO₂ production rates to transpiration changes, and a delayed positive response to
22 GPP.

23 *Conclusions* We found evidence for a combined effect of soil temperature and transpiration that
24 influenced the diel changes in soil CO₂ production. A possible explanation for this pattern could be
25 that a significant part of CO₂ produced in the soil may be transported across soil layers via the
26 xylem.

27 **Keywords** diel timescale, evapotranspiration, gross primary production, soil CO₂ production, time
28 series analysis

29 30 **Introduction**

31 Although evapotranspiration is a key process in ecosystem functioning and has global significance,
32 it was only recently found that it may play a direct and significant role in carbon cycling between
33 the plants and the soil by decreasing root respiration rates (Bekku et al. 2011; Grossiord et al. 2012).
34 Thus, evapotranspiration could have a direct influence on soil CO₂ efflux. Soil CO₂ efflux was
35 typically related to air or soil temperature (T_s), sometimes to soil water content (SWC), and in more
36 recent cases to substrate supply (Lloyd and Taylor 1994; Parkin and Kaspar 2003; Carbone et al.
37 2008; Kuzyakov and Gavrichkova 2010; Balogh et al. 2011). However, abiotic and biotic factors
38 affecting soil CO₂ efflux are acting on different temporal scales and are interacting with each other
39 (Vargas et al. 2010; Savage et al. 2013). Although the need for a proper mechanistic approach to
40 model the effects of the drivers of soil respiration is obvious (Blagodatsky and Smith 2012), the
41 effect of drivers acting on the diel timescale are still poorly understood. New measurement devices
42 and methods, such as soil CO₂ sensors and automated soil respiration systems, provided new

*Corresponding author. Email: balogh.janos@mkk.szie.hu, tel. +3628522075, fax: +3628410804

43 insights into soil carbon fluxes (Carbone and Vargas 2008). These methodological advances
44 allowed measurements of soil CO₂ fluxes with a frequency, which is adequate and necessary for the
45 analysis of diel patterns (Martin et al. 2012; Savage et al. 2013).
46 Previous studies typically focused on the decomposition aspect of soil respiration (F_s) dealing with
47 the effect of T_s and SWC. The effect of T_s on F_s has been extensively studied and used as a basis for
48 soil respiration models in spite of its possible artefacts (Subke and Bahn 2010). The often observed
49 phenomenon of hysteresis in the diel temperature response of soil respiration was usually linked to
50 the different depths of CO₂ production and that of T_s measurements according to a number of
51 studies (Pavelka et al. 2007; Ruehr et al. 2009; Savage et al. 2013; Eler et al. 2013). The hysteresis
52 effect increases the uncertainty of the often applied temperature response of soil or ecosystem
53 respiration, and thus also increases the uncertainties of models and data gap-filling procedures. F_s
54 response to SWC can modify the temperature response, especially in dry ecosystems (Carbone et al.
55 2008; Lellei-Kovács et al. 2011; Fóti et al. 2014). Recent studies proposed parabolic (Moyano et al.
56 2013) or log-normal relationships (Balogh et al. 2011) for describing the effect of SWC, developed
57 principally at low and high water contents (Davidson et al. 2012).
58 Biotic drivers represent the supply-side control in soil respiration models. Biotic drivers that
59 integrate over longer time periods, like biomass, relative growth rate and vegetation indices (Jia and
60 Zhou 2009; Huang and Niu 2012) are useful in describing the phenological changes and
61 physiological state of the vegetation. However, these drivers are not suitable to explain the diel
62 variability of soil respiration. In fact, two additional processes could be relevant on the diel
63 timescale, acting in opposite directions: (1) photosynthesis, and (2) transpiration. Firstly, a time-
64 lagged positive effect of photosynthesis on the respiration of roots and root-associated microbes on
65 the order of hours were found by Mencuccini and Hölttä (2010), who explain this with the increase
66 in easily accessible non-structural hydrocarbon sources for the roots and root-associated organisms.
67 Secondly, it was found that the effect of transpiration could reduce root respiration (Aubrey and
68 Teskey 2009; Bloemen et al. 2013a), and this effect is expected to be immediate (i.e. without
69 hysteretic delay).
70 Removing the effect of the abiotic drivers from the soil efflux signal has helped to clarify the role of
71 other driving variables (Martin et al. 2012). So far, this has been done by multi-temporal correlation
72 approaches (Vargas et al. 2011), by applying better experimental arrangement and data analysis
73 (Graf et al. 2008), and by the proper vertical partitioning of the soil CO₂ production (Davidson et
74 al., 2006). Since the supply-side control on F_s modifies its response to abiotic drivers, this effect
75 could be detected by using residuals of soil respiration models (Balogh et al. 2011).
76 To test this, a combined approach was used in this study. We used automated systems: (i) eddy
77 covariance, (ii) soil respiration, and (iii) soil gradient systems to analyse the effect of the different
78 drivers on the soil CO₂ production and efflux. By measuring CO₂ concentration gradients in three
79 soil layers, source attribution to these layers was possible. A correlation analysis was used to find
80 relationships with gross primary production (GPP) and evapotranspiration (ET), both representing
81 biotic drivers that potentially could significantly influence total soil respiration. Our research goal
82 was to investigate whether and to what extent evapotranspiration modifies observed soil CO₂
83 production and efflux rates in grasslands.

84

85 **Materials and methods**

86 Site characteristics

87 The vegetation at the Bugac site (46.69° N, 19.6° E, 114 m above sea level) is a semi-arid sandy
 88 grassland dominated by *Festuca pseudovina*, *Carex stenophylla* and *Cynodon dactylon*. Mean
 89 annual precipitation of the last ten years (2004-2013) was 575 mm, and the mean annual
 90 temperature reached 10.4 °C. The soil is a chernozem type sandy soil with high organic carbon
 91 content (Table 1).

92 The study site is located in the Kiskunság National Park and has been under extensive management
 93 (grazing) for the last 20 years. The site was grazed occasionally by cattle from the end of April until
 94 the end of November in each year. Grazing pressure was about 0.75 animal ha⁻¹ during the study
 95 period.

96
 97 **Table 1:** Soil characteristics: soil texture, total nitrogen (TN), total organic carbon (TOC), pH, root
 98 biomass, organic matter (OM), bulk density (BD) and total porosity (ϕ). Eight replicates of soil
 99 cores of 15 cm diameter were collected from four depths at the end of the vegetation season on 29th
 100 September 2011.

depth	Sand (%)	Silt (%)	Clay (%)	TN (%)	TOC (%)	pH (KCl)	Root (kg m ⁻³)	OM (%)	BD (g cm ⁻³)	ϕ (m ³ m ⁻³)
0-10	81.18	10.79	8.03	0.19	5.76	7.22	15.15	9.89	0.998	0.605
10-30	81.11	9.62	9.27	0.11	1.32	7.39	9.27	2.21	1.55	0.408
30-50	83.24	7.51	9.24	0.03	0.64	7.92	3.86	1.04	1.59	0.395
50-80	81.42	10.25	8.32	0.01	0.71	8.15	1.51	1.16	1.66	0.37

101

102 Gas exchange measuring systems

103 The three different gas exchange systems used in this study provided data with different levels of
 104 spatial integration; the size of the eddy covariance (EC) flux footprint area was larger by several
 105 orders of magnitude than the area covered by the soil respiration system (SRS) or the gradient
 106 system. The variables derived from EC flux measurements (Fig. 1, GPP, ET) were considered as
 107 biotic drivers of soil CO₂ production rates. Greatest care was taken during the establishment of the
 108 experiment to select a part of the EC footprint area with the same average soil characteristics and
 109 vegetation composition and cover found in the plots where the SRS and gradient systems were
 110 installed. Hence, the GPP and ET estimates obtained in this way can be considered representative
 111 also for the small-scale SRS and gradient system measurements.

112 Data from July 2011 to November 2012 were analysed in this study.

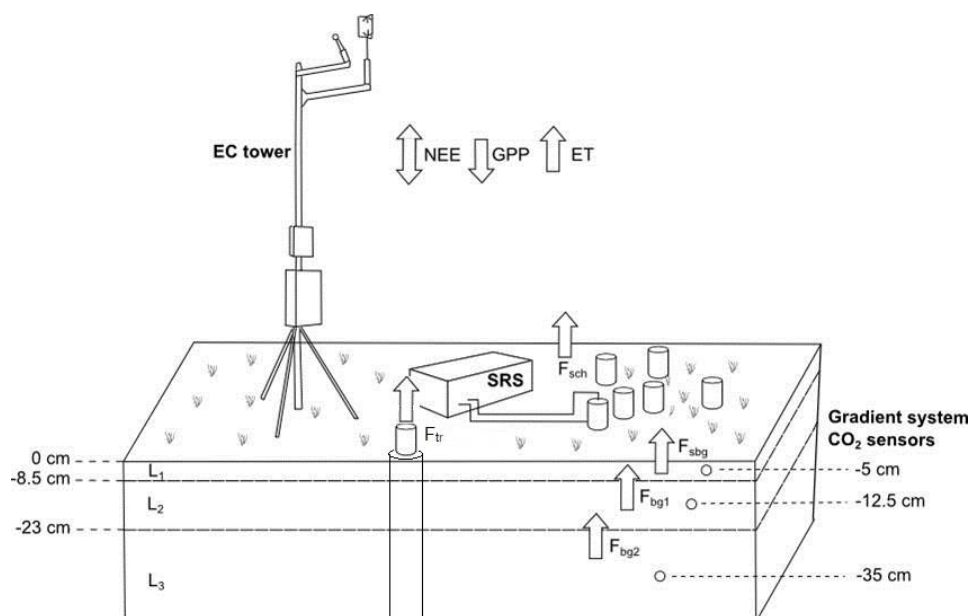
113 *Eddy covariance setup*

114 The EC system at the Bugac site has been measuring the CO₂ and H₂O fluxes continuously since
 115 2002. In dry years this grassland can turn into a net carbon source (Nagy et al. 2007), , but the
 116 long-term annual sums of net ecosystem exchange (NEE) is a small net sink, ranging between -171
 117 and +106 g C m⁻² yr⁻¹ (Pintér et al. 2010).

118 The EC system consists of a CSAT3 sonic anemometer (Campbell Scientific, USA) and a Li-7500
 119 (Licor Inc, USA) open-path infra-red gas analyser (IRGA), both connected to a CR5000 data logger
 120 (Campbell Scientific, USA) via an SDM (synchronous device for measurement) interface.

121 Additional measurements used in this study were: air temperature and relative humidity
 122 (HMP35AC, Vaisala, Finland), precipitation (ARG 100 rain gauge, Campbell, UK), global
 123 radiation (dual pyranometer, Schenk, Austria) incoming and reflected photosynthetically active
 124 radiation (SKP215, Campbell, UK), volumetric soil moisture content (CS616, Campbell, UK) and
 125 soil temperature (105T, Campbell, UK). These measurements were performed as described in Nagy
 126 et al. (2007) and Pintér et al. (2010). Fluxes of sensible and latent heat and CO₂ were processed

127 using an IDL program after Barcza et al. (2003) adopting the CarboEurope IP methodology. For a
 128 detailed description of data processing and gap-filling see Nagy et al. (2007) and Farkas et al.
 129 (2011).



130

131 **Fig. 1** Experimental setup to measure the different gas fluxes within and over the soil. EC tower:
 132 eddy covariance system for measuring net ecosystem exchange of CO₂ (NEE), gross primary
 133 production (GPP), evapotranspiration (ET) and climatic variables. SRS: open soil respiration
 134 system with 6 chambers for the soil surface CO₂ flux measurements (F_{sch}) and 1 chamber for the
 135 trenched plots measurements (F_{tr}). Gradient system: CO₂ sensors inserted into the soil for
 136 measuring soil CO₂ concentration and calculating the following fluxes: CO₂ flux at the soil surface
 137 (F_{sbg}), below-ground CO₂ flux between layer 2 (L₂) and layer 1 (L₁) (F_{bg1}), below-ground CO₂ flux
 138 between layer 3 (L₃) and layer 2 (F_{bg2}).

139 *Soil respiration system*

140 The automated soil respiration system was set up in July 2009. It was upgraded from the 4 chamber
 141 to a 10 chamber version in July 2011. The measurement principle is an open dynamic system
 142 consisting of an SBA-4 infrared gas analyser (PPSystems, UK), pumps, flow meters (D6F-01A1-
 143 110, Omron Co., Japan), electro-magnetic valves, and PVC/metal soil chambers. The chambers
 144 were 10.4 cm high with a diameter of 5 cm, covering a soil surface area of approximately 19.6 cm².
 145 The flow rate through the chambers was 300 ml min⁻¹, which means that the chamber volume is
 146 renewed every 40 seconds. The PVC chambers were enclosed in a white metal cylinder with 2 mm
 147 airspace in between to stabilize the chamber and to prevent warming by direct radiation. Four vent
 148 holes with a total area of 0.95 cm² were drilled in the top of the chambers. Vent holes also served to
 149 allow precipitation to drip into the chambers. The system causes minor disturbance in the soil
 150 structure and the spatial structure of the vegetation. It is applicable without cutting the leaves/shoots
 151 of the plants, so it is not disturbing transport processes (phloem and xylem) taking place within the
 152 plant stems and roots. It is suitable for continuous, long-term unattended measurements of soil CO₂
 153 efflux and has been used in previous experiments (Nagy et al. 2011). The soil respiration chambers
 154 contained no standing aboveground plant material.

155 After each hour of operation, the system was kept idle for the following hour. Six chambers were
 156 used to monitor the total surface CO₂ efflux (F_{sch}) and one chamber for measuring the CO₂ efflux of

157 trenched plots (F_{tr}). This chamber was moved every 2 weeks among the 4 trenched plots, which
158 were installed in 2010. Plastic tubes were used to exclude roots and root-associated microorganisms
159 in these plots. Soil cores (160 mm diameter, 800 mm deep) were drilled and roots were removed
160 from the soil. The soil was put back into the tubes layer by layer. We started our measurements
161 several months after the installation to avoid artefacts from this disturbance. These plots were only
162 used as a standard for the absence of plant physiological effects.

163 Data of the six chambers (F_{sch}) were averaged before analysis. As F_{tr} was measured by only one
164 chamber, but at least twice in one measurement cycle (half an hour), these data were also averaged.
165 Individual measurements were eliminated when the residual of an individual data point was outside
166 the range of the mean \pm three times the standard deviation of the values in a 21-point moving
167 window centered at this data point.

168 The system was tested on a calibration tank (CzechGlobe, Brno, Czech Republic) against known
169 fluxes ($F_{sch} = 0.98 \times F_{cal}$, $r^2=0.92$, $n=86$) and it was also compared to a LI-6400 system at the study
170 site ($F_{sch} = 0.92 \times F_{LI6400}$, $r^2=0.92$, $n=36$).

171

172

173 *Gradient method*

174 The soil CO₂ concentration sensors (gradient system) were installed in June 2009. Three GMP343
175 (Vaisala, Finland) IRGAs were inserted into the soil at depths of 5, 12 and 35 cm, respectively.
176 They were installed in a distance of about 3 m from the eddy station and within 1–2 m from the soil
177 respiration chambers. The sensors were sampled by the CR5000 data logger (also controlling EC
178 measurements) at 10 s intervals and averaged in half-hourly intervals.

179 The CO₂ fluxes measured by the gradient system were compared to those measured by the soil
180 respiration system. Good agreement was found between the two methods ($F_{sbg} = 0.9334 \times F_{sch}$,
181 $r^2=0.61$, $n=3292$).

182 CO₂ fluxes (F_{sbg} , F_{bg1} , F_{bg2}) were calculated according to Moldrup and Olesen (2000) and Davidson
183 et al. (2006). The water retention curve characteristics in the different layers of the investigated soil
184 were taken from a previous study on the water cycle at the study site (Hagyó 2010). CO₂
185 productions in the different layers were calculated as the difference between the incoming and
186 outgoing CO₂ fluxes considering the changes of the CO₂ concentrations in the given layer. For a
187 detailed description of the calculations see the Online Resource.

188

189 *Ancillary measurements*

190 Soil temperatures and volumetric soil water contents were measured at two different depths (5 cm
191 and 30 cm) by the EC system. In order to infer the temperature and soil water content of the
192 intermediate soil layer (L_2), a linear temperature change between the top soil layer (L_1) and the one
193 at 30 cm depth (L_2) was assumed.

194 Broadband Normalized Difference Vegetation Index (NDVI) values were calculated using the
195 incoming and reflected global and photosynthetically active radiation data according to Wang et al.
196 (2004). Daily maximum radiation was used to calculate the daily NDVI values and running average
197 (1 week window size) of these daily NDVI values were then calculated and used for the analysis.

198 Soil pH was determined with the KCl method. Soil bulk density was measured using the volumetric
199 core method at 10 cm depth intervals down to 80 cm. Soil texture was determined according to the
200 Hungarian Standard (MSZ-08-0205:1978). Total organic carbon content (TOC) of the samples was

201 determined by sulfochromic oxidation, total nitrogen content (TN) was determined by the Kjeldahl
202 method (Sparks et al. 1996)

203

204 Soil respiration models

205 Three different soil respiration models were used during the data processing to describe the
206 response of the different CO₂ fluxes and CO₂ production rates to the main abiotic and biotic drivers.
207 In the Lloyd-Taylor (1994) model (model 1) soil temperature is the only driving variable

$$208 \quad F = a \times e^{b \times \left(\frac{1}{56.02} - \frac{1}{T_s - 227.13} \right)} \quad (1)$$

209 where F is the soil CO₂ flux ($\mu\text{mol CO}_2 \text{ m}^{-2} \text{ s}^{-1}$), T_s is the soil temperature at 5 cm in Kelvin, a and b
210 are the model parameters.

211 Model 2 additionally includes SWC (Balogh et al. 2011):

$$212 \quad F = a \times e^{b \times \left(\frac{1}{56.02} - \frac{1}{T_s - 227.13} \right) + \left[-0.5 \times \left[\ln \left(\frac{\text{SWC}}{c} \right) \right]^2 \right]} \quad (2)$$

213 where T_s is the soil temperature at 5 cm in Kelvin, SWC is the volumetric soil water content (%)
214 and a , b and c are the model parameters.

215 Model 3 extended model 2 by adding NDVI (see Section 2.4) as a driving variable:

$$216 \quad F = a \times e^{d \times \text{NDVI} + b \times \left(\frac{1}{56.02} - \frac{1}{T_s - 227.13} \right) + \left[-0.5 \times \left[\ln \left(\frac{\text{SWC}}{c} \right) \right]^2 \right]} \quad (3)$$

217 where T_s is the soil temperature at 5 cm in Kelvin, SWC is the volumetric soil water content (%),
218 NDVI is the normalized difference vegetation index and a , b , c and d are the model parameters.
219 Nonlinear least-squares fitting was done with Sigmaplot 8.0 (SPSS Inc) and IDL (ITT Visual
220 Solutions, USA).

221

222 Time-series analyses of CO₂ productions and fluxes

223 After calculating the CO₂ production rates in the different soil layers we removed the effect of the
224 drivers by subtracting the output of the above described three models from the CO₂ production rates
225 and analysed the residuals from each model to infer the effects of additional, possibly important
226 drivers. The same analysis was done on the CO₂ efflux rates. The model selection procedure was
227 governed by the dictum to use as low a number of predictors as necessary to still obtain a significant
228 model fit.

229 The flowchart in Fig. 2 illustrates the main steps of the analysis. In the first step we used lagged
230 cross-correlation to find the time lag with the temperature, as a phase shift between the measured
231 temperature and CO₂ efflux was often detected (Pavelka et al. 2007; Ruehr et al. 2009). As it is
232 proposed that the time lag between the temperature measured in the upper layer of the soil and the
233 CO₂ production could not be longer than a few hours (Ruehr et al. 2009), we used a 0–6 hour time
234 lag window in our analysis. The time lag within this interval with the correlation maximum was
235 chosen for the next step, using zero lag if no positive correlation was found. We used a 5-day
236 moving window approach.

237 In the second step we fitted the soil respiration models to the measured CO₂ fluxes and CO₂
238 production rates. Model 1 (Eq. 1) and model 2 (Eq. 2) were used first in 5-day long moving
239 window. The model with higher r^2 was used. The r^2 was calculated as: $r^2 = 1 - (\text{residual sum of}$
240 $\text{squares} / \text{total sum of squares})$.

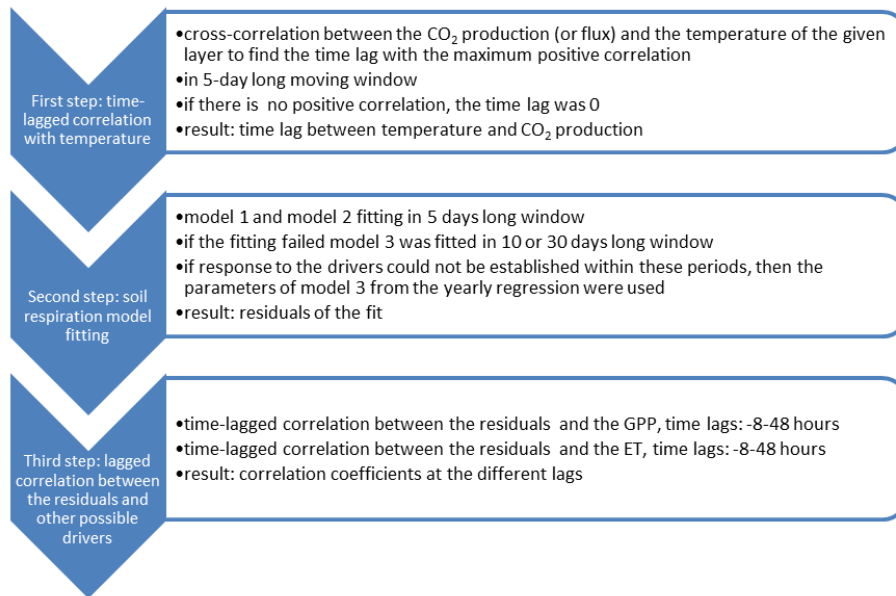
241 If the fit failed (i.e., either r^2 or the parameters were not significantly different from zero), model 3
242 was applied with moving window of 10 days, which – if the fit failed again – was increased to 30
243 days. If the response to the drivers could not be established in the given periods (5, 10, or 30 days),
244 then the parameters of model 3 fitted to the whole dataset were used to calculate the residuals of the
245 fit. The number of cases (days) falling into the different categories are given in the Online
246 Resource.

247 We assumed that the remaining variance after subtracting the effects of T_s , SWC and NDVI could
248 be attributed to the additional drivers, GPP and ET at the diel timescale. This correlation analysis
249 was performed on the whole dataset.

250 The residuals were used in the last step (Fig. 2) to calculate the time-lagged correlation between the
251 residuals and ET and between the residuals and GPP within a time-lag window between –8 and 48
252 hours.

253 Data processing was done in IDL (ITT Visual Solutions, USA).

254



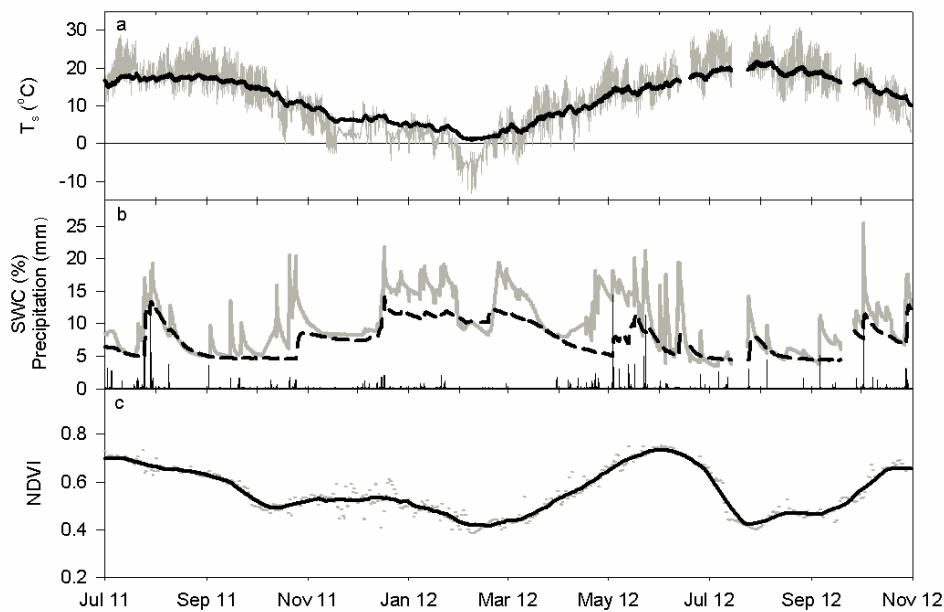
255

256 **Fig. 2** Flowchart of the data analyses steps.

257

258 **Results**

259 Meteorological conditions



260

261 **Fig. 3** Half-hourly (a) soil temperature (T_s) at 5 cm (grey line) and at 30 cm depth (black line), (b)
262 precipitation (bars) and volumetric soil water content (SWC) at 5 cm (grey line) and at 30 cm depth
263 (black line) and (c) broadband NDVI values at maximum radiation (grey dots) and their moving
264 average (black line, window size: 10 days) during the study period (1/7/2011–30/10/2012) at the
265 Bugac site.

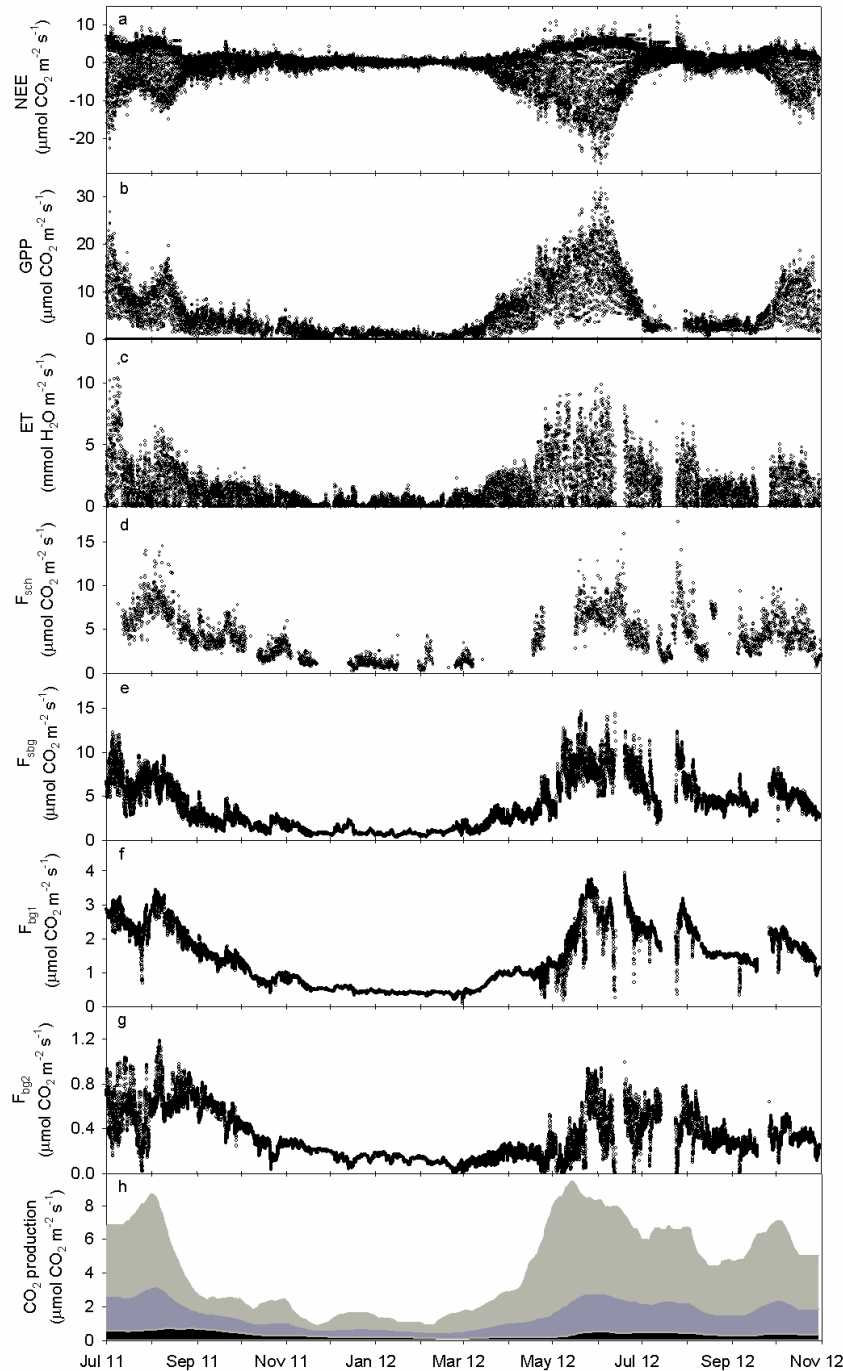
266 The study period of 16 months was dry with 520 mm precipitation in total, which is less than the
267 average annual precipitation. The moisture content of the deeper soil layer was usually lower than
268 that of the upper layer (Fig. 3). This phenomenon clearly shows that there was not enough
269 precipitation to replenish the deeper soil layers, even during the winter. The seasonal change of the
270 NDVI was reflected in the seasonal change of NEE and GPP (Fig. 4a, b). The highest NDVI values
271 were observed at the beginning of June 2012, while the lowest occurred during a drought period at
272 the end of July 2012.

273

274 Annual course of CO₂ fluxes and production in the soil

275 Annual courses of CO₂ and H₂O fluxes were determined by the main drivers (Figs. 3 and 4). The
276 effect of the long, dry autumn of 2011 is shown in Fig. 4 as a continuous decrease in all gas
277 exchange rates from the end of August 2011 until the end of the year. Both CO₂ uptake and CO₂
278 efflux rates were low until the beginning of March 2012. The highest activity was detected in May
279 and June 2012 at time of peak biomass (Fig. 3c). Two active periods could be distinguished in 2012
280 (Fig. 4b): from April to June and in October. There was an extensive drought period in-between,
281 during which the decrease in respiration activity was less pronounced than that in GPP.

282 Sudden declines in below-ground fluxes (Fig. 4f, g) were observed several times during the study
283 period. These cases, when flux rates can drop to zero (e.g. F_{bg2} , in May and June 2012), were
284 observed during precipitation events and resulted in large variances in the below-ground CO₂ fluxes
285 within a short period of time.



286

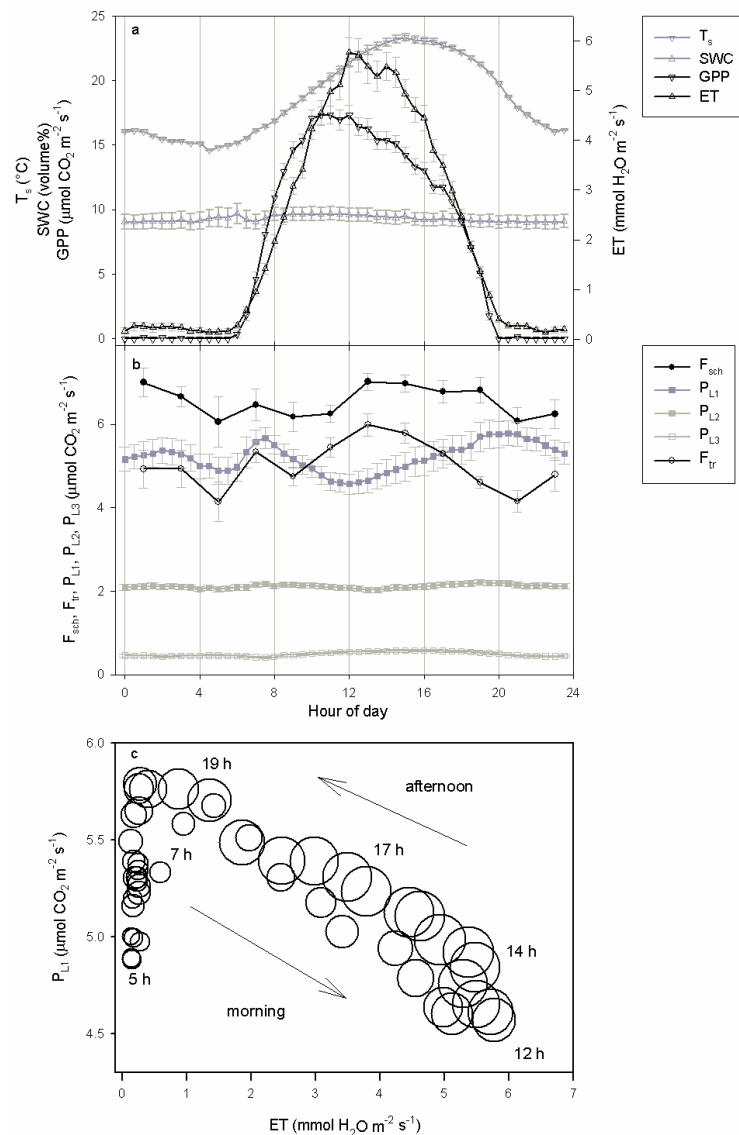
287 **Fig. 4** Seasonal variations of the different half-hourly fluxes as measured by the eddy system (a-c:
 288 NEE, GPP, ET), the soil respiration system (d: F_{sch}) and the gradient system (e-g: F_{sbg} , F_{bg1} , F_{bg2}),
 289 and (h) mean daily CO_2 production in the different layers during the study period at Bugac (grey:
 290 layer 1+2+3, dark grey: layer 2+3, black: layer 3) during the study period (1/7/2011–30/10/2012) at
 291 the Bugac site.

292 The mean daily CO_2 production rates are shown in Fig. 4h. The upper soil layer (L_1) had the highest
 293 CO_2 production during the study period, even during winter, and during the drought in autumn
 294 2011. The minimum and maximum contributions of the different layers to the total daily CO_2
 295 production rates were 30–79%, 18–43% and 2–26% with averages 54%, 33% and 13% in L_1 , L_2
 296 and L_3 , respectively.

297 Diel courses of gas exchange

298 CO₂ production was often lower during daytime than during nighttime. In order to investigate this
 299 phenomenon, half-hourly averages were selected when NDVI values exceeded 0.68 (Fig. 3c) during
 300 the 16 months study period in 2011 and 2012. This selection led to a subset of 58 days. Average
 301 diel courses of CO₂ efflux and production rates, ET, GPP and T_s were then computed from the
 302 selected data (Fig. 5).

303 The average CO₂ production within L₁ (the dominant layer) was lower during much of the day than
 304 during night-time on the selected days. T_s of the layer, however, followed a different course,
 305 peaking during daytime in the late afternoon (Fig. 5a). The average daytime evapotranspiration was
 306 high on the selected days (Fig. 5a).



307

308 **Fig. 5** (a) Average diel courses of soil temperature at 5 cm (T_s), soil moisture at 5 cm (SWC), gross
 309 primary production (GPP) and evapotranspiration (ET) in the active period (NDVI≥0.7) in July-
 310 August 2011 and in May-June 2012 at the Bugac site. (b) Average diel courses of total soil CO₂
 311 efflux (F_{sch}), CO₂ efflux of trenched plots (F_{tr}) and CO₂ production of the three soil layer (P_{L1}, P_{L2},
 312 P_{L3}) in the same period. (c) Average P_{L1} as a function of average ET in the same period. The size of
 313 the circles shows the soil temperature (range: 14.6–23.3 °C). Data of 58 days were averaged, with
 314 error bars showing the standard error.

315

316 Fig. 5b shows the average CO₂ production in the upper layer (P_{L1}) as a function of
 317 evapotranspiration (ET), while the circle size shows soil temperature. With increasing soil
 318 temperatures during the morning and decreasing ones during the night, a counter clockwise
 319 hysteresis of P_{L1} was found. P_{L1} started to decrease after a short rising period (until 7 h) despite the
 320 increasing temperature. In parallel with the temperature ET was increasing until midday. P_{L1} started
 321 to rise only when ET stopped to increase (from 12 h), peaking when ET was close to zero but T_s
 322 was still high (20 h). During the night P_{L1} was decreasing again as well as soil temperature. A
 323 positive correlation with soil temperature was found during the night and at midday (12–14 h),
 324 leading to the observed hysteresis. The minimum CO₂ production rate was 21% lower than the
 325 maximum (4.56 and 5.78 μmol CO₂ m⁻² s⁻¹, respectively), although the maximum was measured at
 326 the lower soil temperature (21.3 and 18.7 °C).

327

328 Time lag between transpiration, C uptake, environmental conditions and respiration losses

329 Summary of model results and residual analysis

330 In the case of F_{sch} the Lloyd-Taylor model (model 1, r²=0.43) gave lower goodness-of-fit value than
 331 the model including the log-normal soil moisture response (model 2, r²=0.56). The incorporation of
 332 NDVI into the soil respiration model improved r² further by 13% (model 3, r²=0.689) (Table 2).

333

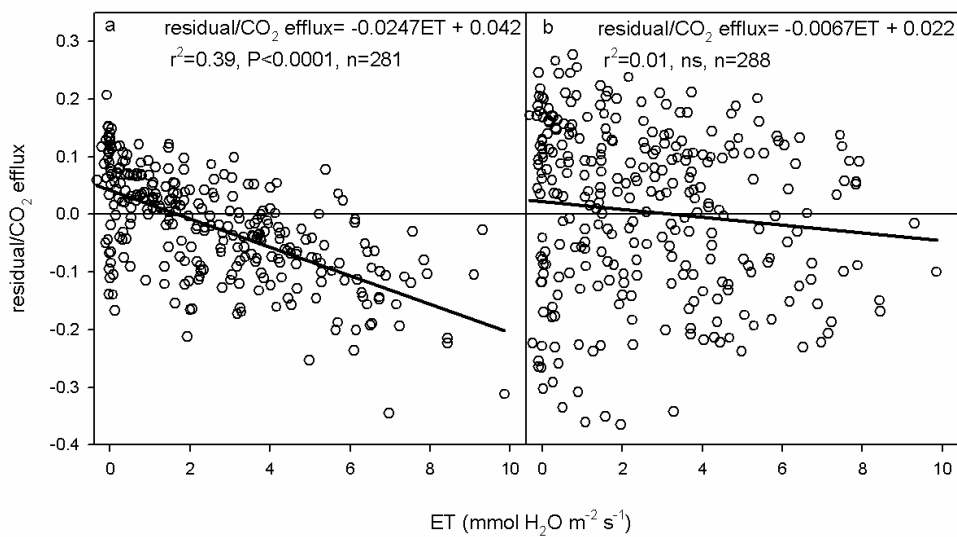
334 **Table 2:** r² values, number of data points (N), coefficients after fitting model 1, 2, 3 (Eq. 1–3) to
 335 half-hourly average soil surface CO₂ fluxes (F_{sch}, F_{tr}), below-ground fluxes (F_{bgs}, F_{bg1}, F_{bg2}) and
 336 CO₂ production rates (P_{L1}, P_{L2}, P_{L3}) of the full study period. Statistical significance levels of the
 337 coefficients and model fitting were P<0.0001 in all cases.

		r ²	N	a	b	c	d
Model 1 $F = a \times e^{b \times \left(\frac{1}{56.02} - \frac{1}{T_s - 227.13} \right)}$	F _{sch}	0.431	3590	2.53	161.55	-	-
	F _{tr}	0.5	3349	1.89	194.96	-	-
	F _{sbg}	0.54	22032	2.21	246.6	-	-
	F _{bg1}	0.68	22032	0.99	236.2	-	-
	F _{bg2}	0.19	22020	0.15	242.01	-	-
	P _{L1}	0.38	21807	0.76	273.4	-	-
	P _{L2}	0.67	21999	0.72	262.9	-	-
	P _{L3}	0.35	21954	0.17	281.07	-	-
Model 2 $F = a \times e^{b \times \left(\frac{1}{56.02} - \frac{1}{T_s - 227.13} \right) + \left[-0.5 \times \left[\ln \left(\frac{SWC}{c} \right) \right]^2 \right]}$	F _{sch}	0.555	3544	2.99	208.05	12.43	-
	F _{tr}	0.479	3349	2.17	195.76	13.08	-
	F _{sbg}	0.58	22032	2.62	308.1	14.34	-
	F _{bg1}	0.7	22032	1.08	233.3	8.03	-
	F _{bg2}	0.49	22020	0.303	189.19	6.08	-
	P _{L1}	0.48	21807	1.85	418.39	31.7	-
	P _{L2}	0.69	21999	0.79	297.9	10.74	-
	P _{L3}	0.505	21954	0.26	279.16	7.8	-
Model 3 $F = a \times e^{d \times NDVI + b \times \left(\frac{1}{56.02} - \frac{1}{T_s - 227.13} \right) + \left[-0.5 \times \left[\ln \left(\frac{SWC}{c} \right) \right]^2 \right]}$	F _{sch}	0.689	3544	0.58	177.65	11.85	2.93
	F _{tr}	0.555	3349	0.53	169.57	12.76	2.5
	F _{sbg}	0.665	22032	0.383	231.23	12.33	3.42
	F _{bg1}	0.812	22032	0.258	181.46	6.95	2.66
	F _{bg2}	0.58	22030	0.083	268.17	6.31	1.98
	P _{L1}	0.495	21184	0.38	216.67	14.79	3.12
	P _{L2}	0.751	21185	0.224	234.25	9.69	2.48
	P _{L3}	0.58	21184	0.085	315.07	7.54	1.84

338

339

340 The average soil CO₂ efflux measured at the surface (F_{sch}) showed no correlation with average ET
 341 nor with the average soil temperature in the active period when NDVI values exceeded 0.68, even
 342 when a time lag of up to 5 hours was considered, while fluxes from the vegetation removal
 343 treatment (F_{tr}) showed best correlation with temperature at 0 hours time lag (data not shown). We
 344 however had expected that the effect of ET on P_{L1} should also be found in the surface soil CO₂
 345 efflux, therefore we asked the question whether this effect can be seen in the residuals. We used
 346 model 3 to remove the effect of the main abiotic drivers from the whole dataset. For F_{sch} residuals a
 347 significant negative correlation was found with ET during the active periods, selected by high
 348 NDVI values (≥ 0.68). Contrastingly, no correlation was found between F_{tr} residuals and ET for the
 349 same period.



350

351 **Fig. 6** Standardized residuals of (a) surface CO₂ efflux (F_{sch}) and (b) trenched plots without roots
 352 (F_{tr}) as a function of ET values in the active periods with NDVI ≥ 0.68 . The linear regressions are
 353 shown (solid line).

354

355 To quantify the effect of ET on soil respiration rates, standardized flux residuals were plotted as a
 356 function of ET. At low ET values, F_{sch} was 5% higher than predicted by the model. At high ET
 357 rates, the measured F_{sch} was significantly lower than predicted (-10 to -20% at $ET > 6$ mmol H₂O
 358 m⁻² s⁻¹). Overall, the difference between the standardized residuals at low and high
 359 evapotranspiration rates was about 0.2, which means a 20% difference compared to the measured
 360 CO₂ effluxes (Fig. 6a).

361

362 *Results of time-series analyses*

363 Correlations between F_{sch}, P_{L1-3} and abiotic (T_s, SWC) and biotic drivers (ET, GPP) were further
 364 analysed with time-series analyses of the whole dataset in order to reveal the detailed diel and
 365 seasonal correlations.

366 Time lagged correlations between F_{sch}, P_{L1-3} and T_s were calculated in the first step of our analyses
 367 (cf. Fig. 2) using moving windows of 5 days length. No consistent time lag was found between the
 368 two variables. In the case of F_{sch} the correlation coefficient was statistically significant in 158 out of
 369 the 345 cases (days), with a zero lag being the most frequent time lag (92 cases or 58% of these
 370 cases). Cases with significant correlations were uniformly distributed over the study period with no
 371 seasonal preference (data not shown).

372 Time lagged correlation was further analysed both with ET and GPP for the full study period.
373 Residuals were calculated after subtracting the main effects of soil temperature, soil water content
374 and NDVI (Fig. 2) from F_{sch} and P_{L1-3} rates. These residuals were then correlated with ET and GPP.
375 As the time lags of the significant correlations were not normally distributed, we calculated the
376 mode of the time lags for F_{sch} and the CO_2 production in the different layers.
377 Strong negative correlations between the residuals and ET were found mostly between -2 and 5
378 hours time lag in the upper two layers, but with longer time lags in the third layer (Online Resource
379 Fig. 2 b-d). Approximately 12–16 hours after the negative correlation peak there was a positive
380 correlation in all cases. The annual course of the significant correlations shows that the time lag of
381 the negative correlations slightly changes during the year (Online Resource Fig. 2). There was no
382 clear diel pattern during winter. The modes of time lags of the significant negative correlations for
383 F_{sch} , P_{L1} , P_{L2} and P_{L3} , respectively were at 1.5, 0.5, 0.5, 4.5 hours.
384 In the case of the GPP we assumed that the positive correlation maximum represents the connection
385 between GPP and CO_2 production. Positive significant correlations could be found during the whole
386 study period, but the correlation coefficient was lower than that with ET (Online Resource Fig. 2 e–
387 h). The modes of the time lags of the significant positive correlations for F_{sch} , P_{L1} , P_{L2} and P_{L3} ,
388 respectively were at 15, 11, 18, 20 hours.

389

390 Discussion

391 Annual course of CO_2 fluxes and production in the soil

392 The seasonal courses of the CO_2 fluxes followed the changes of the main environmental drivers, as
393 temperature (as well as incoming radiation) and the amount of soil water available to plants. There
394 were differences between the two autumns studied: the second half of 2011 was very dry, the soil
395 CO_2 production rates in autumn 2012 were two times the rates observed in autumn 2011 (Fig. 4).
396 Significant rain events affected the belowground CO_2 fluxes negatively, especially the below-
397 ground fluxes (Fig. 4). The observed decline (even down to zero) in these fluxes was mainly caused
398 by the indirect effect of precipitation: the increasing CO_2 concentration due to the enhanced
399 respiratory activity on excess moisture in the upper soil layers decreased, or even reversed the
400 normal CO_2 gradient within the soil (Nagy et al. 2011).

401 The distribution of the CO_2 production rates along the three soil layers corresponded well with our
402 expectations. It was expected that the upper layer would be the most significant in contributing to
403 total CO_2 efflux (Davidson et al., 2006; Verma and Kelleners, 2012), since it contains the majority
404 of active roots and associated microbial communities (Subke and Bahn 2010) as well as the
405 majority of the fresh SOM. In spite of the highly variable water supply, the upper layer was the
406 main contributor to the total CO_2 efflux even under drought conditions (Fig. 4).

407 Diel courses of gas exchange

408 CO_2 production rates were often found to be higher during the night than during daytime (Fig. 5a)
409 in the active periods. Several factors that could be the reason for this phenomenon were considered.
410 Since highest CO_2 concentrations up to 1400 ppm at 10 cm above ground level are found during
411 nights with no wind, or low wind velocity, the question is whether these high concentrations in the
412 air are actually rather a result of CO_2 advection from surrounding areas which would then be
413 erroneously interpreted as higher apparent productivity in the soil. If this were the case, then we
414 would expect an apparently positive correlation between calculated soil CO_2 production (as a direct
415 function of measured CO_2 concentration in the soil), and soil temperature, based on the fact that

416 soils tend to cool less under calm and low wind speed conditions, and consequently temperature
417 stays highest in these periods. Our data, however, show the opposite: a significantly negative
418 correlation between P_{L1} and CO_2 concentration at 10 cm during nights of the active period. This
419 finding also excludes the potential interpretation that soil temperatures remain warmer during calm
420 nights (which would result in increased P_{L1}) than during more turbulent nights.
421 Alternatively, the increase of both autotrophic and heterotrophic respiration due to water
422 redistribution from deeper layers to the dry surface soil layer (Carbone et al. 2008; Ruehr et al.
423 2009), could explain the higher nighttime production. However, the water content of the upper
424 layers showed no significant changes during the day (0.7 % on average during the selected period
425 with $NDVI \geq 0.68$) as would be required to maintain this hypothesis. Another explanation could be
426 increased water availability during the night and especially in the early morning when the surface
427 water content can be increased by dew formation. But this phenomenon possibly only affects the
428 uppermost layer (litter and the surface of the soil) and is unlikely to influence deeper layers.
429 From this we conclude that it may not be the increase in respiration at night that needs further
430 attention, but the decrease in respiration during the day. It was recently found that transpiration can
431 modify the apparent autotrophic CO_2 production by the transport of CO_2 in the xylem of trees
432 (Grossiord et al. 2012; Bloemen et al. 2013a; Bloemen et al. 2013b). Therefore, the transpiration
433 should be considered as a factor potentially affecting apparent soil CO_2 production, not only in
434 trees, but also in grasses, herbs and forbes. CO_2 produced in the soil that equilibrates with the CO_2
435 in the xylem stream in the roots bypasses the conventional soil chamber measurements, and thus we
436 can hypothesize that a negative correlation with a short time lag should be found between
437 respiration processes and ET. Our measurements are in agreement with this hypothesis: a negative
438 correlation was found between P_{L1} and ET. P_{L1} was correlated with soil temperature at night and
439 during midday (12–14h) when ET was almost constant. Contrastingly, during times with little
440 temporal changes in T_s but relevant changes in ET (e.g. during the afternoon, 14–19 h) a negative
441 correlation between P_{L1} and ET led to the hysteresis loop seen in Figure 5c. These two factors
442 seemed to govern the changes in P_{L1} during the entire day. The short rising period of P_{L1} in the early
443 morning could be attributed to the temperature changes, but when ET became significantly higher
444 (more than $1 \text{ mmol H}_2\text{O m}^{-2} \text{ s}^{-1}$) P_{L1} started falling. Another turning point was with decreasing ET
445 during late afternoon: P_{L1} was rising to its maximum after ET started to decline, despite the
446 decreasing temperature. Our results show that P_{L1} was lowered by about 20% due to the effect of
447 transpiration. No correlation was found between F_{sch} and T_s , nor ET. However, F_{tr} was positively
448 correlated with both T_s and ET. This difference indirectly shows the significance of living roots in
449 the soils and their potential to modify soil CO_2 efflux via transpiration.

450 Time lag between evapotranspiration, C uptake, environmental conditions and respiration losses

451 *Summary of model results and residual analysis*

452 The Lloyd-Taylor soil respiration model extended by a log-normal function of soil moisture and by
453 an exponential function of NDVI was able to properly describe the response of soil respiration to
454 these drivers at our site. The log-normal shape of soil moisture-respiration response was proposed
455 before (Balogh et al. 2011; Moyano et al. 2013). It originated from the Michaelis-Menten kinetics
456 of the response of respiration to substrate and oxygen availability (Davidson et al. 2012). The
457 incorporation of NDVI into the soil respiration model improved the explanatory power of the model
458 similarly to the findings of Huang and Niu (2012). As the reflectance and greenness of the surface
459 change with the phenological changes of the vegetation, photosynthesis-related vegetation indices

460 can be used to estimate the effect of CO₂ uptake on respiration (Huang et al. 2012), or even the ratio
461 of root-derived CO₂ in ecosystem respiration (Wang et al. 2010), so it can be incorporated into soil
462 respiration models (Huang and Niu 2012).

463 After subtracting the effect of the main drivers by fitting model 3 we found a significant negative
464 correlation between the residuals of the soil respiration rates and ET when NDVI was high. The
465 difference between soil respiration at low and at high transpiration rates could reach as much as
466 20% as compared to the measured rates. Similar results were obtained when only the CO₂
467 production of the upper layer was considered (Fig. 5). The effect is not so high as it was found for
468 trees (Aubrey and Teskey 2009), but still it was significant, hence it should be considered in soil
469 CO₂ production models. This suggests that calculations and modelling based on daytime
470 measurements in the active periods could significantly underestimate the real CO₂ production of the
471 soil.

472

473 *Results of time-series analyses*

474 Contrary to the findings of other studies (Davidson et al. 2006b; Vargas et al. 2010), there was no
475 consistent time lag between soil temperature and soil CO₂ efflux, neither at higher, nor at lower soil
476 water contents (data not shown). The most frequent time lag with significant correlation between
477 soil temperature and soil CO₂ efflux (F_{sch}) was 0 hours and the average lag time of significant
478 correlations was 1.15 hours. These time lags are in good agreement with the CO₂ production rates,
479 which can be explained by the upper layer (0-8 cm) being the main contributor to the total CO₂
480 efflux with the calculated diffusion rates.

481 Several studies (e.g. Moyano et al. 2007; Kuzyakov and Gavrichkova 2010; Hopkins et al. 2013)
482 proposed CO₂ uptake (GPP) as a driver of soil (root) respiration, while others (e.g. Aubrey and
483 Teskey 2009; Bloemen et al. 2013a) stated that the transpiration has a major effect on the diel
484 variability of soil CO₂ efflux. The daily courses of transpiration and GPP are very similar due to the
485 stomatal co-regulation of both processes (Hetherington and Woodward 2003). Therefore, it could be
486 difficult to separate the two effects. In this study, we found similar time-lagged correlations of CO₂
487 production with ET and GPP, but the correlations were stronger in the case of ET during the whole
488 study period.

489 The effect of CO₂ uptake can be significant according to girdling studies (Högberg et al. 2001;
490 Jones et al. 2009), but it can be assumed that its effect on the diel variability can be less pronounced
491 due to the longer turnover time of soluble carbohydrates compared to diel changes (Högberg et al.
492 2008). Moreover, starch accumulation during the day ensures the continuous carbohydrate export
493 from leaves to non-photosynthetic tissues at night, avoiding large fluctuations on diel scale (Lu et
494 al. 2005; Mencuccini and Hölttä 2010).

495 But the effect of ET is expected to be instantly: root water uptake should keep pace with
496 transpiration (Aston and Lawlor 1979), especially in herbaceous plants where the role of
497 capacitance is probably minor as compared to trees (Högberg and Read 2006). In this study, a
498 shorter time lag was found in the response to ET (0.5 hour time lag in the upper soil layers)
499 compared to a longer one with GPP (11–18 hours in the upper soil layers). The latter corresponds
500 well with an average a time lag of 12.5 hours between CO₂ uptake and soil respiration found by
501 different studies in grasslands, while this time lag increased to 22 hours if only field studies were
502 considered (Kuzyakov and Gavrichkova 2010).

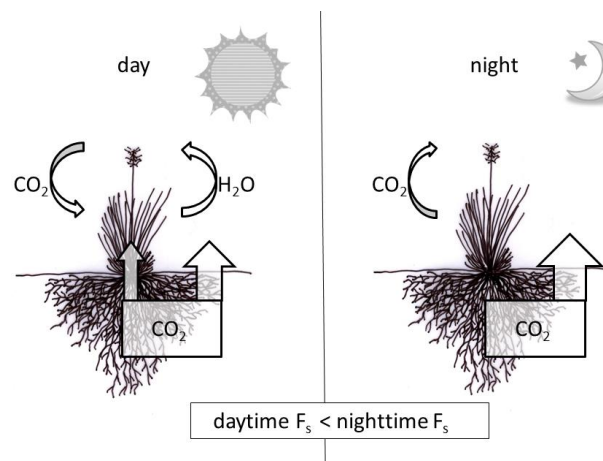
503 Further, the time lags of the peak correlation changed during the study period. Longer time lags for
504 ET and GPP were obtained in the most active periods for all layers. This can be explained by the

505 fact that transport routes of carbon and water get longer as the shoot and the root systems become
506 longer in the course of the season (Mencuccini and Hölttä 2010). The same effect could be
507 important in deeper layers: the longer the route within the plant, the longer the time lags between
508 the physiological processes.

509

510 Implications for soil and ecosystem respiration measurements

511 According to our results, soil CO₂ production could be decreased by 20% due to the effect of
512 evapotranspiration (Fig. 7) in the active periods. Since manual soil respiration measurements are
513 usually made during daytime due to practical reasons, response functions to environmental drivers
514 derived from these measurements could underestimate the all-day CO₂ efflux. Given the amount of
515 CO₂ emitted through the soil to the atmosphere is lower during daytime due to the xylem-
516 transported CO₂, but does it have any effect on the calculations of ecosystem respiration (R_{eco})?
517 Daytime R_{eco} estimations are usually based on the temperature response observed at night
518 (Reichstein et al. 2005), thus when the soil CO₂ efflux to the atmosphere has shown to be higher at
519 our site. However we should consider that the transpiration stream does not affect the amount of
520 CO₂ produced under the surface, our results only suggest that the transport route could be different
521 at daytime and nighttime. Therefore it can be assumed that this phenomenon has no influence on
522 GPP estimations in grasslands. Bloemen et al. (2013b) found that most of the xylem-transported
523 CO₂ was respired to the atmosphere through stem and branch efflux in trees. However, the
524 important difference between herbaceous plants and trees in this respect is that the transport route is
525 shorter and that the xylem sap CO₂ transport happens in the vicinity of the photosynthetic tissues.
526 Therefore the re-fixation of the xylem-transported CO₂ is more likely in herbaceous plants.
527 Our results showed a nice example how the different gas fluxes are tightly coupled in the soil-
528 vegetation-atmosphere system. Soil respiration models considering this phenomenon could be able
529 to explain a large part of diel variation and improve the goodness of annual sum estimations and
530 GPP partitions.



531

532 **Fig. 7** The difference between daytime and nighttime soil respiration processes in grasslands: a
533 significant part of the CO₂ produced in the soil could be transported via transpiration stream and
534 assimilated in the plant during daytime.

535 Conclusions

536 Three automated techniques of CO₂ gas exchange measurements were used to quantify the effects
537 of principal biotic and abiotic factors on soil CO₂ production on different (from diel to annual)
538 timescales. We found that besides temperature and soil moisture, transpiration was controlling the

539 diel course of the CO₂ production. After subtracting the effects of the main abiotic drivers we found
540 strong negative correlations between evapotranspiration and soil CO₂ production rates, and less
541 strong, but still significant positive correlations between gross CO₂ uptake and soil CO₂ production.
542 Since our results suggest that the daytime CO₂ production measurements in grasslands could be
543 underestimated due to the CO₂ transport in the xylem, our findings strongly suggest that the effect
544 of transpiration should be considered both in soil respiration models and in field measurement
545 protocols.

546 Our results provide further evidence of a potential hidden CO₂ transport within the plants, which is
547 not measured by traditional CO₂ gas exchange techniques. Estimations of soil CO₂ production and
548 GPP would hence benefit from explicit consideration of this phenomenon.

549 **Acknowledgements**

550 The authors gratefully acknowledge the financial support of the projects OTKA-PD 100575,
551 OTKA-PD 100944, Research Centre of Excellence (8526-5/2014/TUDPOL) and AnimalChange
552 (FP7 266018). János Balogh acknowledges the support of the János Bolyai Research Scholarship of
553 the Hungarian Academy of Sciences and a Sciex-NMS-CH scholarship, grant #12.043. Szilvia Fóti
554 acknowledges the support of the János Bolyai Research Scholarship of the Hungarian Academy of
555 Sciences.

556

557 **References**

- 558 Aston MJ, Lawlor DW (1979) The Relationship between Transpiration, Root Water Uptake and
559 Leaf Water Potential. *J Exp Bot* 30:169–181.
- 560 Aubrey DP, Teskey RO (2009) Root-derived CO₂ efflux via xylem stream rivals soil CO₂ efflux.
561 *New Phytol* 184:35–40. doi: 10.1111/j.1469-8137.2009.02971.x
- 562 Balogh J, Pintér K, Fóti S, et al. (2011) Dependence of soil respiration on soil moisture, clay
563 content, soil organic matter, and CO₂ uptake in dry grasslands. *Soil Biol Biochem* 43:1006–
564 1013. doi: 10.1016/j.soilbio.2011.01.017
- 565 Barcza Z, Haszpra L, Kondo H (2003) Carbon exchange of grass in Hungary. *Tellus B* 187–196.
- 566 Bekku Y, Sakata T, Tanaka T, Nakano T (2011) Midday depression of tree root respiration in
567 relation to leaf transpiration. *Ecol Res* 26:791–799. doi: 10.1007/s11284-011-0838-z
- 568 Blagodatsky S, Smith P (2012) Soil physics meets soil biology: Towards better mechanistic
569 prediction of greenhouse gas emissions from soil. *Soil Biol Biochem* 47:78–92. doi:
570 10.1016/j.soilbio.2011.12.015
- 571 Bloemen J, McGuire MA, Aubrey DP, et al. (2013a) Transport of root-respired CO₂ via the
572 transpiration stream affects aboveground carbon assimilation and CO₂ efflux in trees. *New*
573 *Phytol* 197:555–65. doi: 10.1111/j.1469-8137.2012.04366.x
- 574 Bloemen J, McGuire MA, Aubrey DP, et al. (2013b) Assimilation of xylem-transported CO₂ is
575 dependent on transpiration rate but is small relative to atmospheric fixation. *J Exp Bot*
576 64:2129–38. doi: 10.1093/jxb/ert071
- 577 Carbone MS, Vargas R (2008) Automated soil respiration measurements: new information,
578 opportunities and challenges. *New Phytol* 177:297–300. doi: 10.1111/j.1469-
579 8137.2007.02336.x
- 580 Carbone MS, Winston GC, Trumbore SE (2008) Soil respiration in perennial grass and shrub
581 ecosystems: Linking environmental controls with plant and microbial sources on seasonal and
582 diel timescales. *J Geophys Res* 113:G02022. doi: 10.1029/2007JG000611

583 Davidson E, Savage K, Trumbore S, Borken W (2006a) Vertical partitioning of CO₂ production
584 within a temperate forest soil. *Glob Chang Biol* 12:944–956. doi: 10.1111/j.1365-
585 2486.2006.01142.x

586 Davidson EA, Janssens IA, Luo Y (2006b) On the variability of respiration in terrestrial
587 ecosystems: moving beyond Q₁₀. *Glob Chang Biol* 12:154–164. doi: 10.1111/j.1365-
588 2486.2005.01065.x

589 Davidson EA, Samanta S, Caramori SS, Savage K (2012) The Dual Arrhenius and Michaelis-
590 Menten kinetics model for decomposition of soil organic matter at hourly to seasonal time
591 scales. *Glob Chang Biol* 18:371–384. doi: 10.1111/j.1365-2486.2011.02546.x

592 Eler K, Plestenjak G, Ferlan M, et al. (2013) Soil respiration of karst grasslands subjected to
593 woody-plant encroachment. *Eur J Soil Sci* 64:210–218. doi: 10.1111/ejss.12020

594 Farkas C, Alberti G, Balogh J, et al. (2011) Methodologies. In: Haszpra L (ed) *Atmospheric
595 Greenhouse Gases: The Hungarian Perspective*. Springer, New York, pp 65–90

596 Fóti S, Balogh J, Nagy Z, et al. (2014) Soil moisture induced changes on fine-scale spatial pattern
597 of soil respiration in a semi-arid sandy grassland. *Geoderma* 213:245–254. doi:
598 10.1016/j.geoderma.2013.08.009

599 Graf A, Weihermüller L, Huisman J, et al. (2008) Measurement depth effects on the apparent
600 temperature sensitivity of soil respiration in field studies. *Biogeosciences* 5:1175–1188.

601 Grossiord C, Mareschal L, Epron D (2012) Transpiration alters the contribution of autotrophic and
602 heterotrophic components of soil CO₂ efflux. *New Phytol* 194:647–53. doi: 10.1111/j.1469-
603 8137.2012.04102.x

604 Hagyo A (2010) *Vízforgalom gyep és erdő területeken (Water cycle of grasslands and forests)*. PhD
605 Thesis, Szent István University, p.129.

606 Hetherington AM, Woodward FI (2003) The role of stomata in sensing and driving environmental
607 change. *Nature* 424:901–908.

608 Höglberg P, Höglberg MN, Göttlicher SG, et al. (2008) High temporal resolution tracing of
609 photosynthate carbon from the tree canopy to forest soil microorganisms. *New Phytol*
610 177:220–8. doi: 10.1111/j.1469-8137.2007.02238.x

611 Höglberg P, Nordgren A, Buchmann N, et al. (2001) Large-scale forest girdling shows that current
612 photosynthesis drives soil respiration. *Nature* 411:789–92. doi: 10.1038/35081058

613 Höglberg P, Read DJ (2006) Towards a more plant physiological perspective on soil ecology.
614 *Trends Ecol Evol* 21:548–54. doi: 10.1016/j.tree.2006.06.004

615 Hopkins F, Gonzalez-Meler MA, Flower CE, et al. (2013) Ecosystem-level controls on root-
616 rhizosphere respiration. *New Phytol* 199:339–51.

617 Huang N, Niu Z (2012) Estimating soil respiration using spectral vegetation indices and abiotic
618 factors in irrigated and rainfed agroecosystems. *Plant Soil* 367:535–550. doi: 10.1007/s11104-
619 012-1488-9

620 Huang N, Niu Z, Zhan Y, et al. (2012) Relationships between soil respiration and photosynthesis-
621 related spectral vegetation indices in two cropland ecosystems. *Agric For Meteorol* 160:80–89.
622 doi: 10.1016/j.agrformet.2012.03.005

623 Jia B, Zhou G (2009) Integrated diurnal soil respiration model during growing season of a typical
624 temperate steppe: Effects of temperature, soil water content and biomass production. *Soil Biol
625 Biochem* 41:681–686. doi: 10.1016/j.soilbio.2008.12.030

626 Jones DL, Nguyen C, Finlay RD (2009) Carbon flow in the rhizosphere: carbon trading at the soil-
627 root interface. *Plant Soil* 321:5–33. doi: 10.1007/s11104-009-9925-0

628 Kuzyakov Y, Gavrichkova O (2010) Review: Time lag between photosynthesis and carbon dioxide
629 efflux from soil: a review of mechanisms and controls. *Glob Chang Biol* 16:3386–3406. doi:
630 10.1111/j.1365-2486.2010.02179.x

631 Lellei-Kovács E, Kovács-Láng E, Botta-Dukát Z, et al. (2011) Thresholds and interactive effects of
632 soil moisture on the temperature response of soil respiration. *Eur J Soil Biol* 47:247–255. doi:
633 10.1016/j.ejsobi.2011.05.004

- 634 Lloyd J, Taylor J (1994) On the temperature dependence of soil respiration. *Funct Ecol* 8:315–323.
- 635 Lu Y, Gehan J, Sharkey T (2005) Daylength and circadian effects on starch degradation and
636 maltose metabolism. *Plant Physiol* 138:2280–2291. doi: 10.1104/pp.105.061903.2280
- 637 Martin JG, Phillips CL, Schmidt A, et al. (2012) High-frequency analysis of the complex linkage
638 between soil CO₂ fluxes, photosynthesis and environmental variables. *Tree Physiol* 32:49–64.
639 doi: 10.1093/treephys/tpr134
- 640 Mencuccini M, Hölttä T (2010) The significance of phloem transport for the speed with which
641 canopy photosynthesis and belowground respiration are linked. *New Phytol* 185:189–203. doi:
642 10.1111/j.1469-8137.2009.03050.x
- 643 Moldrup P, Olesen T (2000) Predicting the gas diffusion coefficient in undisturbed soil from soil
644 water characteristics. *Soil Sci Soc Am J* 64:94–100.
- 645 Moyano F, Kutsch W, Schulze E (2007) Response of mycorrhizal, rhizosphere and soil basal
646 respiration to temperature and photosynthesis in a barley field. *Soil Biol Biochem* 39:843–853.
647 doi: 10.1016/j.soilbio.2006.10.001
- 648 Moyano FE, Manzoni S, Chenu C (2013) Responses of soil heterotrophic respiration to moisture
649 availability: An exploration of processes and models. *Soil Biol Biochem* 59:72–85. doi:
650 10.1016/j.soilbio.2013.01.002
- 651 Nagy Z, Pintér K, Czóbel S, et al. (2007) The carbon budget of semi-arid grassland in a wet and a
652 dry year in Hungary. *Agric Ecosyst Environ* 121:21–29. doi: 10.1016/j.agee.2006.12.003
- 653 Nagy Z, Pintér K, Pavelka M, et al. (2011) Carbon balance of surfaces vs. ecosystems: advantages
654 of measuring eddy covariance and soil respiration simultaneously in dry grassland ecosystems.
655 *Biogeosciences* 8:2523–2534. doi: 10.5194/bg-8-2523-2011
- 656 Parkin TB, Kaspar TC (2003) Temperature Controls on Diurnal Carbon Dioxide Flux : Implications
657 for Estimating Soil Carbon Loss. *Soil Sci Soc Am J* 67:1763–1772.
- 658 Pavelka M, Acosta M, Marek M V., et al. (2007) Dependence of the Q₁₀ values on the depth of the
659 soil temperature measuring point. *Plant Soil* 292:171–179. doi: 10.1007/s11104-007-9213-9
- 660 Pintér K, Balogh J, Nagy Z (2010) Ecosystem scale carbon dioxide balance of two grasslands in
661 Hungary under different weather conditions. *Acta Biol Hung* 61 Suppl:130–5. doi:
662 10.1556/ABiol.61.2010.Suppl.13
- 663 Reichstein M, Falge E, Baldocchi D, et al. (2005) On the separation of net ecosystem exchange into
664 assimilation and ecosystem respiration: review and improved algorithm. *Glob Chang Biol*
665 11:1424–1439. doi: 10.1111/j.1365-2486.2005.001002.x
- 666 Ruehr NK, Knohl A, Buchmann N (2009) Environmental variables controlling soil respiration on
667 diurnal, seasonal and annual time-scales in a mixed mountain forest in Switzerland.
668 *Biogeochemistry* 98:153–170. doi: 10.1007/s10533-009-9383-z
- 669 Savage K, Davidson E a., Tang J (2013) Diel patterns of autotrophic and heterotrophic respiration
670 among phenological stages. *Glob Chang Biol* 19:1151–1159. doi: 10.1111/gcb.12108
- 671 Sparks D, Page A, Helmke P, et al. (1996) Methods of soil analysis - Part 3: Chemical methods.
672 1309.
- 673 Subke J-A, Bahn M (2010) On the “temperature sensitivity” of soil respiration: Can we use the
674 immeasurable to predict the unknown? *Soil Biol Biochem* 42:1653–1656.
- 675 Vargas R, Baldocchi DD, Bahn M, et al. (2011) On the multi-temporal correlation between
676 photosynthesis and soil CO₂ efflux: reconciling lags and observations. *New Phytol* 191:1006–
677 17. doi: 10.1111/j.1469-8137.2011.03771.x
- 678 Vargas R, Detto M, Baldocchi DD, Allen MF (2010) Multiscale analysis of temporal variability of
679 soil CO₂ production as influenced by weather and vegetation. *Glob Chang Biol* 16:1589–1605.
680 doi: 10.1111/j.1365-2486.2009.02111.x
- 681 Verma AK, Kelleners TJ (2012) Depthwise Carbon Dioxide Production and Transport in a
682 Rangeland Soil. *Soil Sci Soc Am J* 76:821–828. doi: 10.2136/sssaj2011.0416

- 683 Wang Q, Tenhunen J, Dinh NQ, et al. (2004) Similarities in ground- and satellite-based NDVI time
684 series and their relationship to physiological activity of a Scots pine forest in Finland. *Remote*
685 *Sens Environ* 93:225–237. doi: 10.1016/j.rse.2004.07.006
- 686 Wang W, Peng S, Fang J (2010) Root respiration and its relation to nutrient contents in soil and root
687 and EVI among 8 ecosystems, northern China. *Plant Soil* 333:391–401. doi: 10.1007/s11104-
688 010-0354-x
- 689